METHODS

Animals. For genetic mapping, *plt*/+ heterozygotes were crossed with strain CAST/Ei (Jackson Laboratory). Experiments were carried out on F_2 and F_3 mice from the mapping cross. This research was approved by the University of Michigan Committee on Use and Care of Animals. Animals were housed and cared for in accordance with NIH guidelines.

Genotyping and markers. Genotyping was carried out using microsatellite markers from public databases as well as novel microsatellite markers designed from mouse genomic sequence (http://www.ensemble.org). D10Umi13 was amplified with the forward primer 5′-CCACCACATCAACAGGCTCACAGG and the reverse primer 5′-AATGCAACCGTGACACAAGTACAC. PCR was carried out with the PCR core kit (Qiagen). PCR products were separated on 6% acrylamide gels and stained with ethidium bromide. The pale tremor mutation is genotyped by PCR with a forward primer in intron 18 (5′-CGTATGAATTGAGTAGTTTTGATG) and two reverse primers, one in the proximal LTR of the inserted *ETn2β* element (5′-GCTGGGGGAGGGGAGACTACACAG) and one in exon 19 (5′-ATGGACTTGGATCAATGCCAACAG).

RT–PCR. Total RNA was isolated from brain of P7 mice, before extensive neurodegeneration. cDNA was synthesized using the First Strand cDNA Synthesis Kit (Invitrogen). RT–PCR was carried out with the PCR Core Kit (Qiagen). Long-range PCR was performed with the Expand Long Template PCR System (Roche). The northern blot with 3 μg of polyA$^+$ RNA was prepared as previously described[28]. The hybridization probe, a 1 kb RT–PCR product containing exons 8 to 15, was labelled with two radiolabelled nucleotide triphosphates.

Histology. Tissues were sectioned and stained at HistoServ. Fast blue/eosin staining was carried out in the Department of Pathology, University of Michigan. Light microscopy was performed on an Olympus BX-51 microscope and DP50 camera. Sciatic and femoral nerves were sectioned and stained with osmium for electron microscopy as previously described[27]. Skin whole mounts were prepared from P10 mice with the guidance of A. Dlugosz. The commercial depilatory Nair was applied to the dorsal surface for five minutes followed by washing with warm water to remove hair. The skin was dissected and superficial fascia removed. Follicles were visualized on a standard dissecting microscope with transmitted light.

Neurophysiology. Nerve conduction velocities were recorded from affected pale tremor mice and littermate controls. Mice were anaesthetized with a ketamine/xylazine solution and placed under a heating lamp to maintain body temperature at 32 °C. Recordings were obtained using a Nicolet VikingQuest portable system and Nicolet disposable EEG needles. Tail sensory responses were obtained by stimulating proximally over a 3 cm region. Sciatic nerve motor velocities were obtained by stimulating distally at the sciatic notch and proximally at the knee.

Cell culture and immunofluorescence. Primary fibroblasts were cultured from mouse tail biopsies treated with collagenase. Cells were plated in DMEM with 10% fetal bovine serum, and maintained at 37 °C with 5% CO_2 for up to three passages. For immunofluorescence, 100,000 cells were seeded on polylysine-coated cover slips in 35 mm dishes. We thank T. August and the Developmental Studies Hybridoma Bank for monoclonal antibody to LAMP-2, developed under the auspices of the NICHD and maintained by the Department of Biological Sciences, University of Iowa. For labelling with antibody, cells were fixed with ice-cold methanol at –20 °C for 5 min and blocked with 2% goat serum. Antibodies were applied for 1 h in PBS with 2% serum at room temperature and detected with Alexa Fluor 488 donkey anti-rabbit (Molecular Probes) or Alexa Fluor 594 goat anti-rat (Molecular Probes). Cells were visualized on a DeltaVision Deconvolution microscope system (Applied Precision).

Hippocampal neurons were cultured with glial conditioned media. Neurons were visualized with a Nikon TE2000 microscope.

Phosphoinositide assays. Fibroblast phosphoinositides were labelled with myo-[2-^{3}H] inositol, extracted and quantified by HPLC. Mouse fibroblasts from the first passage were grown in 100 mm dishes to 60–70% confluency. The culture was rinsed with PBS and starved for 12 h in inositol-free DMEM (Tissue Culture Support Centre, Washington University) supplemented with 5 μg ml^{-1} transferrin, 5 μg ml^{-1} insulin and 10% dialysed fetal bovine serum. The medium was replaced with labelling medium (inositol-free DMEM containing 5 μg ml^{-1} transferrin, 20 mM HEPES and 50 μCi myo-[2-^{3}H] inositol, GE Healthcare). After 24 h, the culture was treated with 0.6 ml of 4.5% (v/v) perchloric acid for 15 min, scraped off the plate, and spun down at 12,000*g* for 10 min at 4 °C. The pellet was washed with 0.1 M EDTA once and resuspended in 50 μl deionized water. To deacylate the lipids, samples were transferred to a glass vial, mixed with 1 ml methanol/40% methylamine/*n*-butanol (4:4:1, v/v), and incubated at 55 °C for 1 h. The resulting samples were vacuum-dried, resuspended in 0.3 ml water and extracted twice with an equal volume of *n*-butanol/ethyl ether/formate (20:4:1, v/v). The aqueous phase was vacuum dried and resuspended in 20 μl water.

For separation of all isoforms of the glycerophosphoinositides by HPLC, two different elution gradients were used at 1 ml min^{-1} flow rate. (Pump A, H_2O; pump B, 1 M $(NH_4)_2HPO_4$, pH 3.8.) Gradient 1: 0% B for 5 min; 0–2% B over 15 min; 2% B for 80 min; 2–12% B over 20 min; 12% B for 20 min; 12–80% B over 40 min; 80% B for 20 min; 80–0% B over 5 min. To separate glyceroPtdIns(3,4)P_2 from glyceroPtdIns(3,5)P_2, a longer gradient (gradient 2) was used: 0% B for 5 min; 0–2% B over 15 min; 2% B for 80 min; 2–10% B over 20 min; 10% B for 65 min; 10–80% B over 40 min; 80% B for 20 min; 80–0% B over 5 min. The positions of glyceroPtdIns(3)P, glyceroPtdIns(3,5)P_2, glyceroPtdIns(3,4)P_2 and glyceroPtdIns(3,4,5)P_3 were determined by ^{32}P-labelled standards received as gifts from L. Rameh. The positions of glyceroPtdIns(4)P and glyceroPtdIns(4,5)P_2 were confirmed with yeast glycerophosphoinositide extracts.

Human mutation detection. The cohort of unrelated patients with CMT disorder was previously described[13]. The clinical diagnosis was based on clinical examination, electrophysiological studies and, in a few cases, nerve biopsy. All patients received appropriate counselling and gave informed consent approved by the institutional review board. For the initial screen of *FIG4*, each coding exon was amplified and examined by heteroduplex analysis as previously described[25]. The patient mutations were identified by sequencing products exhibiting abnormal mobility. Subsequently, the 23 exons of *FIG4* were completely sequenced from the four individuals carrying variants.

Supplementary Materials

Supplementary Video: Movement disorder in *plt* mice
A video showing the typical movement disorder displayed by *plt* mice. 4 week old mouse.

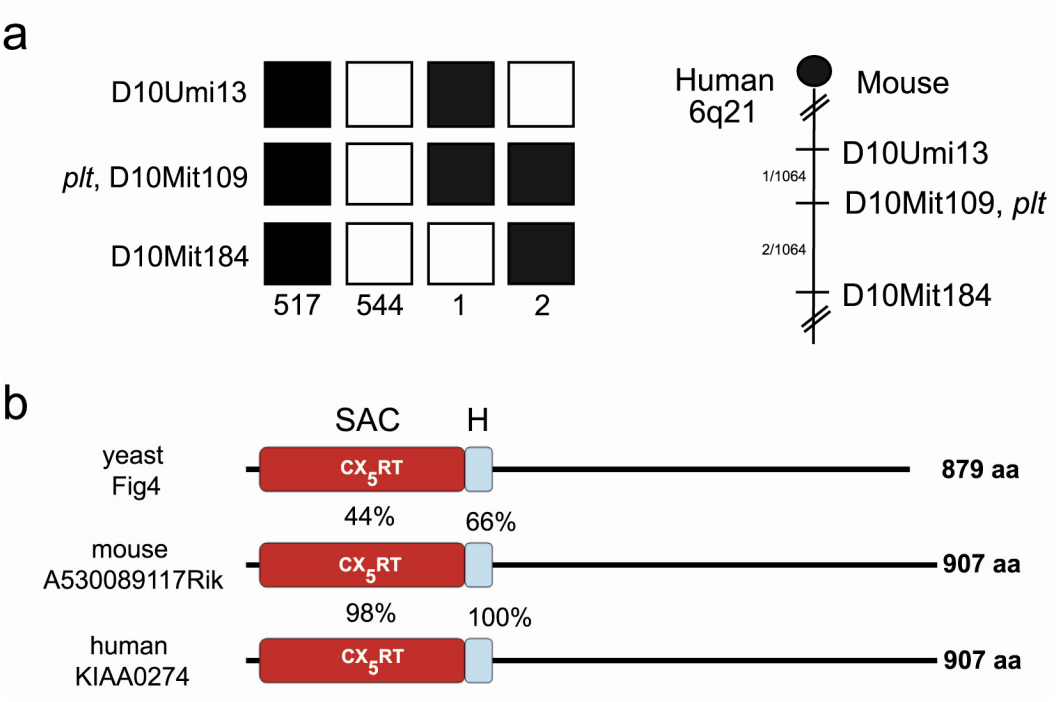

Supplementary Figure 1: Positional cloning of the *pale tremor* gene.
a, Genetic mapping of *plt* on mouse chromosome 10. The haplotypes of 3 recombinant chromosomes and 1,061 nonrecombinant chromosomes are indicated; solid symbols represent alleles from inbred strains; open symbols represent CAST alleles. The 2 Mb nonrecombinant interval of mouse chromosome 10 between D10Umi13 and D10Mit184 is shown at the right. **b,** Protein domains of yeast Fig4p and mammalian homologs. See text for description of the SAC phosphatase domain.

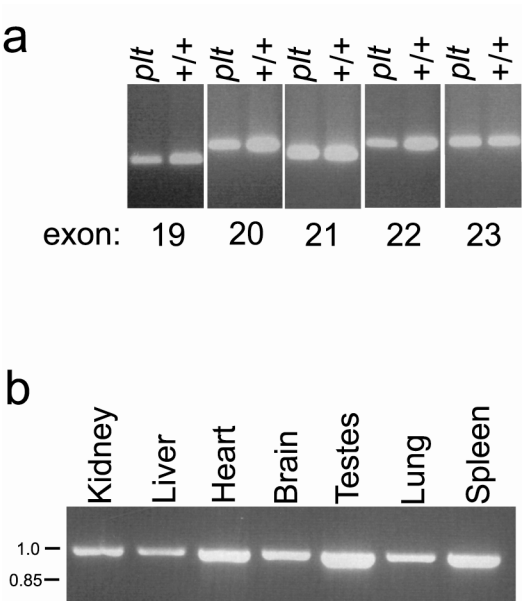

Supplementary Figure 2: Molecular characterization of *plt* mutation and *Fig4* expression.
a, PCR of genomic DNA using primers flanking exons 19 through 23. **b,** RT-PCR of the *Fig4* transcript from wildtype tissues; primers located in exon 8 and exon 15.

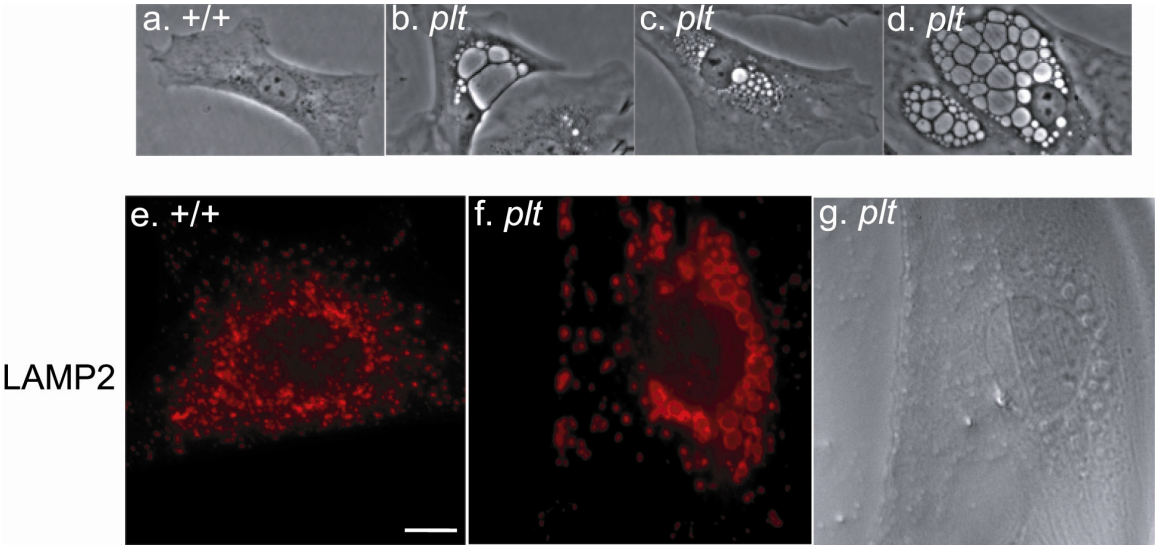

Supplementary Figure 3: Cytoplasmic vesicles in cultured fibroblasts from *pale tremor* mice.
a-d, Mutant fibroblasts are filled with vacuoles. **e-g,** Membranes of large cytoplasmic vesicles stain with antiserum to LAMP2, a lysosomal membrane protein. Scale bar: 10 μm

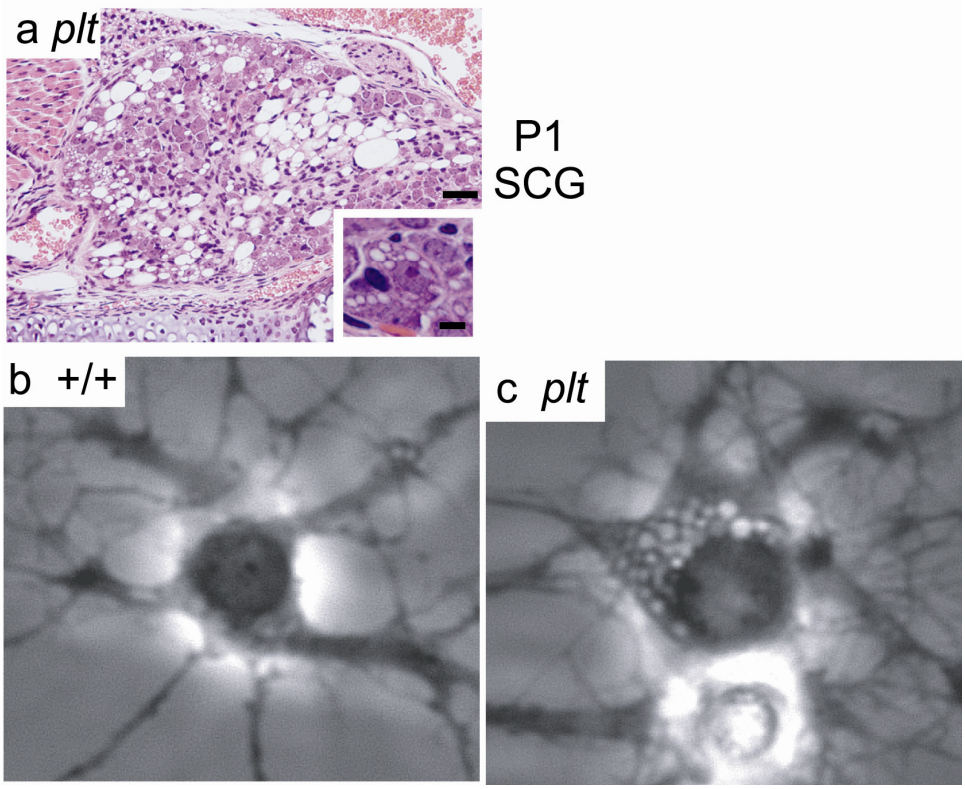

Supplementary Figure 4: Neuropathology in *plt* mice.
a, Superior cervical ganglion at P1. **b-c,** Cultured hippocampal neurons from E16.5 embryos. Tissue sections were stained with hematoxylin and eosin (**a**). Scale bar: 25 microns for panels, 12.5 microns for insets

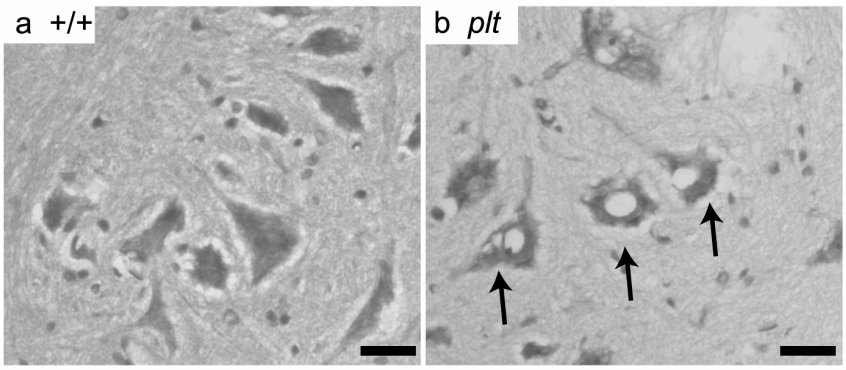

Supplementary Figure 5: Vesicle accumulation in motor neurons from 5 wk old mice.
H&E staining was performed on the spinal cord sections from wild-type and mutant mice. **a.** Typical motor neurons were visualized in the anterior horn of the spinal cord from wild-type mice. **b.** In the mutant spinal cord, a majority of motor neurons contained vacuoles scattered in the cytoplasm (arrows), similar to neurons in DRG and brain. Scale bar = 25 microns.

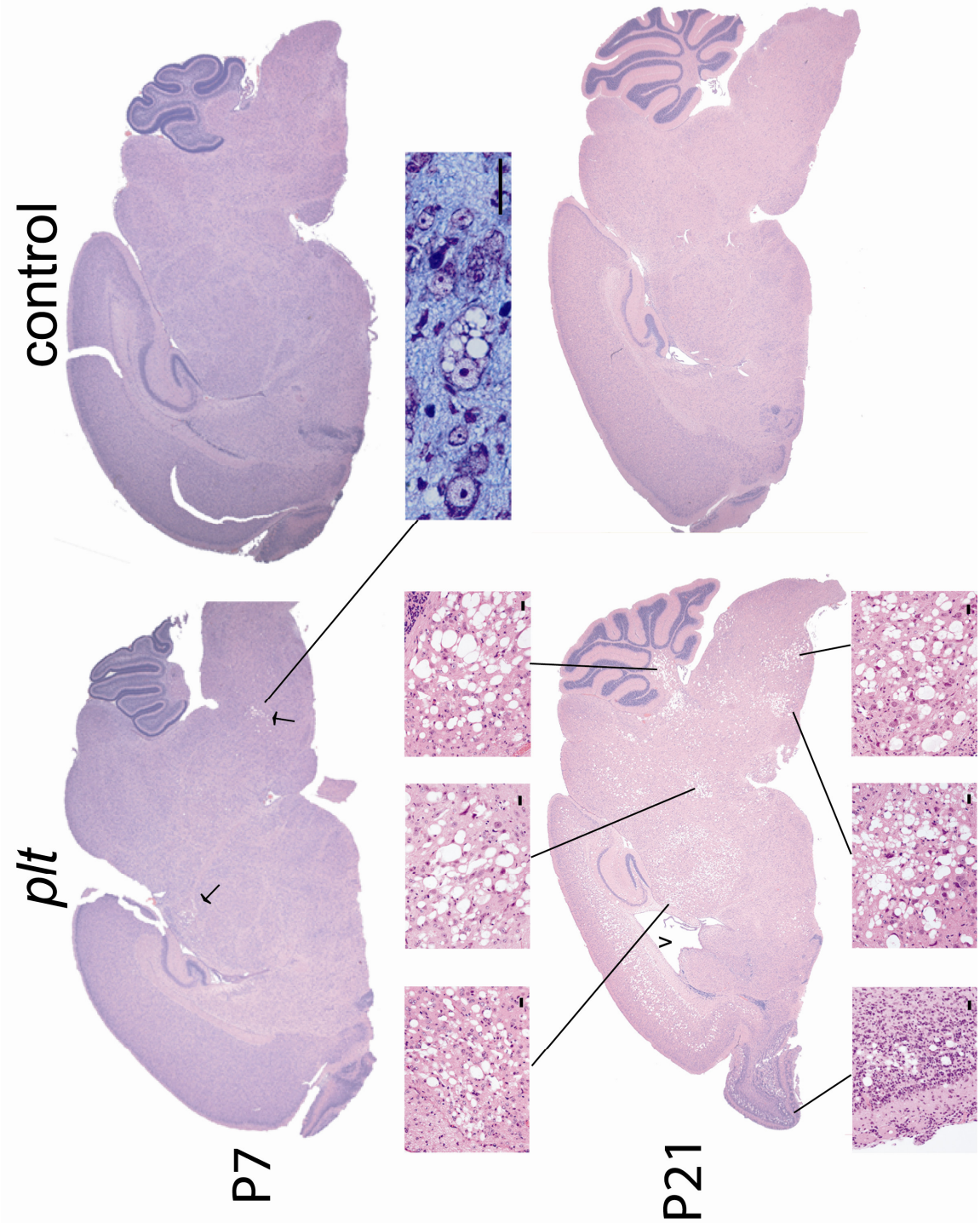

Supplementary Figure 6: Brain degeneration in *pale tremor* mice.
Sagittal sections of brain from wildtype and mutant littermates at 1 and 3 weeks of age. High magnification views of neuronal cell bodies from regions of degeneration are shown in the inserts. Tissue sections were stained with hematoxylin and eosin or luxol fast blue and hematoxylin. V, ventricle. Scale bars: 25 microns.

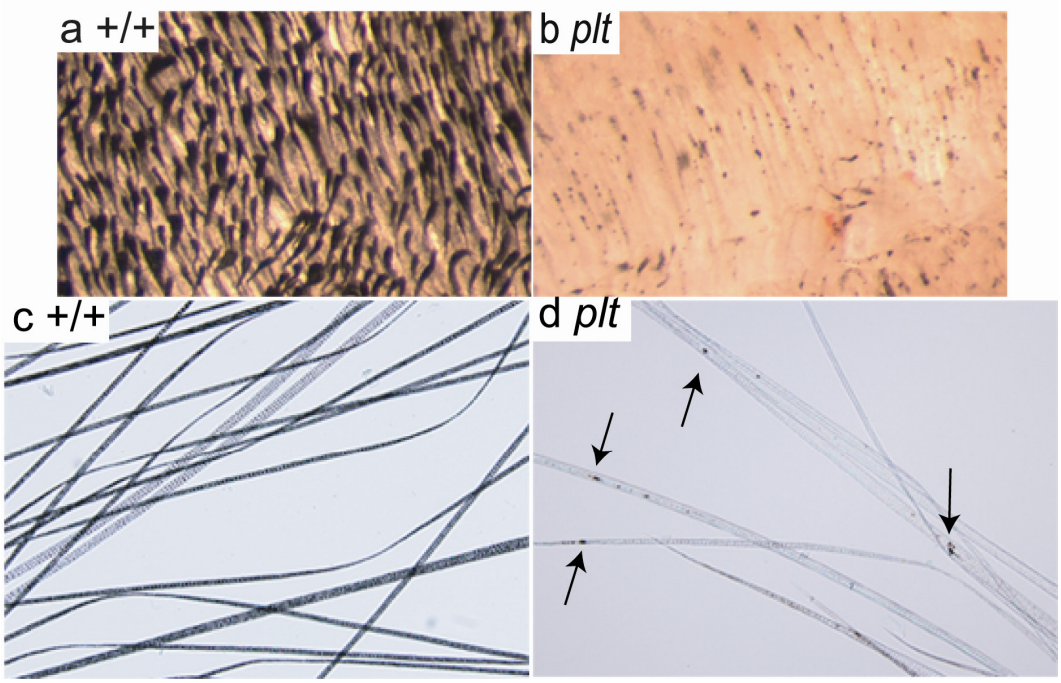

Supplementary Figure 7: Pigment abnormalities in *plt* mice
a-b, Skin wholemounts from P10 mice demonstrating pigment-containing hair follicles. Original magnification: 8.5X. **c-d,** Melanosome clumping in mutant hair shafts (arrows). Original magnification: 10X

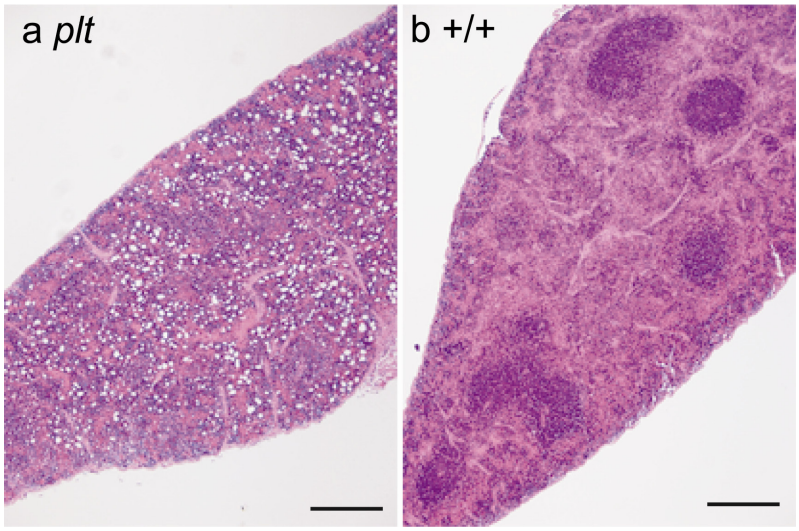

Supplementary Figure 8: Spleen pathology in *plt* mice
plt (**a**) and wt (**b**) spleens from 3 week old animals. H&E. scale bar: 250 microns.

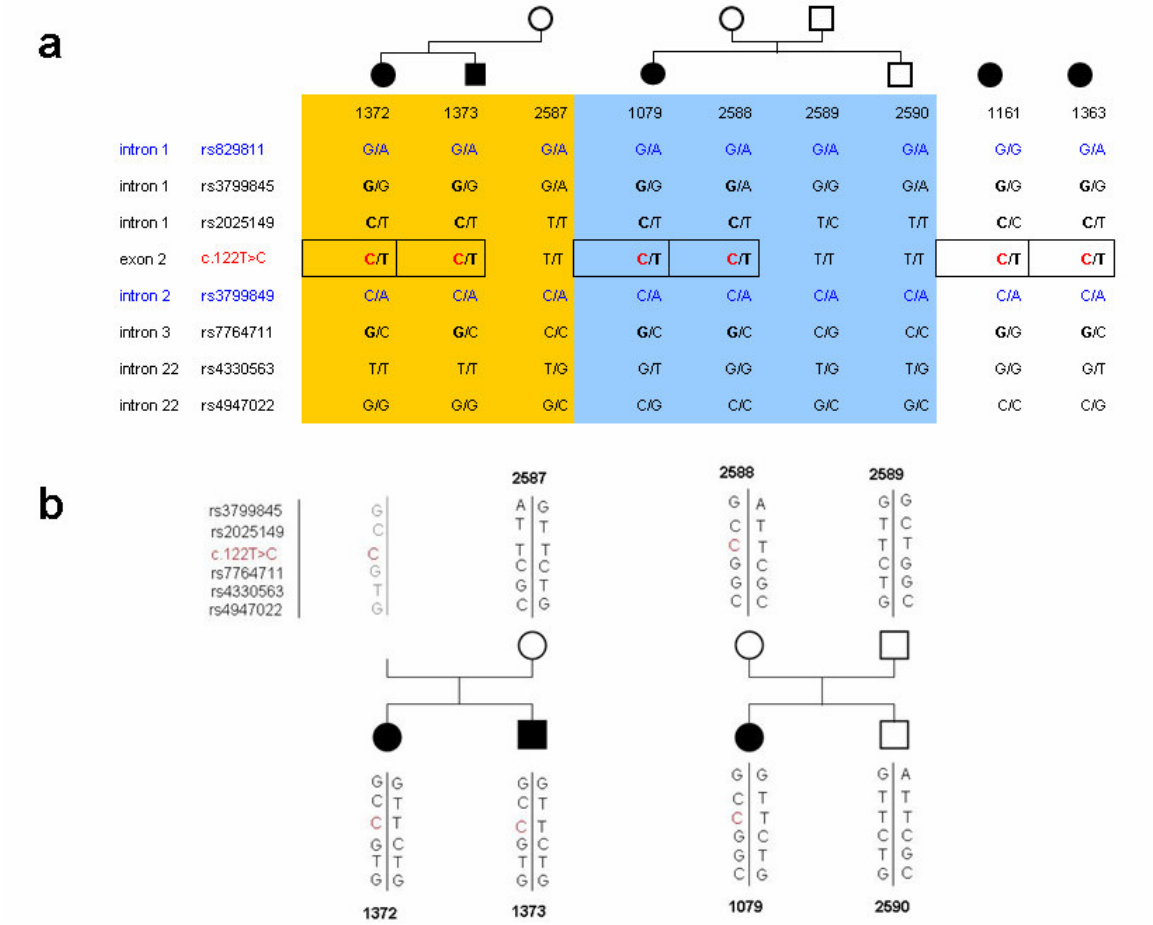

Supplementary Figure 9. Haplotypes of CMT patients with mutations in FIG4.

a. Genotypes. Seven SNPs from the HapMap database, and the Ile41Thr mutation (c.122T>C) were genotyped for patients and family members. **b.** Haplotypes. The five SNPs shown in black were informative in the two available pedigrees and permitted reconstruction of the haplotypes. The Ile41Thr (c.122T>C) allele is carried by the same haplotype in all four patients. The Ile41Thr allele has a calculated LD coefficient D' equal to 1 for rs3799845, rs2025149 and rs7764711. D' equals 0.11 for rs4330563 and rs4947022.

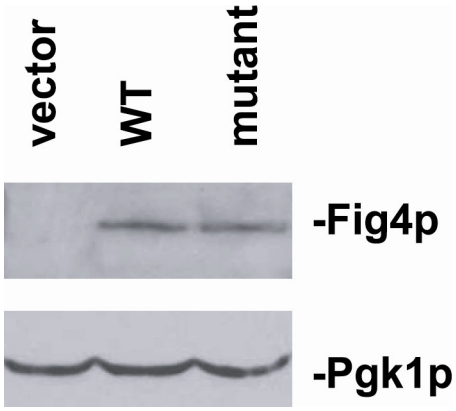

Supplementary Figure 10: The FIG4 allele Ile>Thr is defective in activation of yeast Fab1/PIKfyve.
The fig4Δ yeast strain lacking endogenous Fig4p was transformed with wildtype myc-Fig4 (WT) or mutant myc-Fig4 containing the I59T substitution that corresponds to human I41T (mutant), or with empty vector. **a.** Western blot analysis with anti-myc antibody demonstrates comparable expression of wildtype and mutant protein.

Supplementary Discussion

CMT type 4B1 is caused by mutations in myotubularin related protein 2 (*MTMR2*), a 3-phosphatase that can catalyze *in vitro* dephosphorylation of PI(3)P and PI(3,5)P_2[14, 16]. Mutations of *MTMR2* are predicted to increase the levels of PI(3,5)P_2 but the actual effect of these mutations on phosphoinositide levels has not been experimentally determined. The clinical effects of mutations in MTMR2 are much less severe than the *FIG4* mutations described here[15, 17], suggesting that these enzymes may function in different subcellular compartments or exhibit distinct substrate specificities *in vivo*. CMT Type 4B2 is caused by mutations in MTMR13/SBF2[18], an enzymatically inactive protein that interacts with MTMR2. CMT4G was recently found to result from mutations in frabin/FGD4, a Rho GTPase guanine nucleotide exchange factor[19]. frabin/FGD4 contains PH and FYVE domains which interact with specific phosphoinositides.